

# SCUBA observations of dust around Lindroos stars: evidence for a substantial submillimetre disc population

M. C. Wyatt,<sup>\*</sup> W. R. F. Dent and J. S. Greaves

*UK Astronomy Technology Centre, Royal Observatory, Blackford Hill, Edinburgh EH9 3HJ*

Accepted 2003 March 1. Received 2003 February 27; in original form 2002 November 21

## ABSTRACT

We have observed 22 young stars from the Lindroos sample at 850  $\mu\text{m}$  with SCUBA on the James Clerk Maxwell Telescope to search for evidence of dust discs. Stars in this sample are the less massive companions of B-type primaries and have well-defined ages that are 10–170 Myr; i.e. they are about to, or have recently arrived on the main sequence. Dust was detected around three of these stars (HD 112412, 74067 and 99803B). The emission around HD 74067 is centrally peaked and is approximately symmetrically distributed out to  $\sim 70$  arcsec from the star. This emission arises from either a two-component disc, one circumstellar and the other circumbinary with dust masses of 0.3 and  $>27 M_{\oplus}$ , respectively, or an unrelated background object. The other two detections we attribute to circumsecondary discs with masses of 0.04 and  $0.3 M_{\oplus}$ . We were also able to show that a circumpriary disc is present around HD 112413 with a similar mass to that around the companion HD 112412. Cross-correlation of our sample with the *IRAS* catalogues only showed evidence for dust emission at 25 and 60  $\mu\text{m}$  toward one star (HD 1438); none of the submillimetre detections were evident in the far-infrared data implying that these discs are cold ( $<40$  K assuming  $\beta = 1$ ). Our submillimetre detections are some of the first of dust discs surrounding evolved stars that were not detected by *IRAS* or *ISO* and imply that 9–14 per cent of stars could harbour previously undetected dust discs that await discovery in unbiased sub-mm surveys. If these discs are protoplanetary remnants, rather than secondary debris discs, dust lifetime arguments show that they must be devoid of small  $<0.1$  mm grains. Thus it may be possible to determine the origin of these discs from their spectral energy distributions. The low inferred dust masses for this sample support the picture that protoplanetary dust discs are depleted to the levels of the brightest debris discs ( $\sim 1 M_{\oplus}$ ) within 10 Myr, although if the extended emission of HD 74067 is associated with the star, this would indicate that  $>10 M_{\oplus}$  of circumbinary material can persist until  $\sim 60$  Myr and would also support the theory that T Tauri discs in binary systems are replenished by circumbinary envelopes.

**Key words:** binaries: visual – circumstellar matter – planetary systems: protoplanetary discs – stars: pre-main-sequence – submillimetre.

## 1 INTRODUCTION

Most, if not all, stars are born with a disc of gas and dust (e.g. Shu, Adams & Lizano 1987). The fate of such protoplanetary discs is important, since it is within these discs that planets are thought to form through the coagulation of initially submicron-sized dust grains (Weidenschilling & Cuzzi 1993; Lissauer 1993). Such grain growth is expected to continue as long as the parent disc remains sufficiently massive and models show that the terrestrial planets of our solar system could have achieved a sizeable fraction of their final mass by this mechanism within 10 Myr (e.g. Lissauer 1993).

However, at the same time as grain growth is occurring several other mechanisms are competing to deplete disc material. These mechanisms include: viscous gas drag and Poynting–Robertson light drag, both of which result in the accretion of disc material on to the star; stripping of disc material by a stellar wind and radiation pressure; removal of material during encounters with nearby stars; and photo-evaporation, either by the parent star or by an external star (Clarke, Gendrin & Sotomayor 2001; Hollenbach, Yorke & Johnstone 2000). Clearly, the success or otherwise of planet formation depends on whether this process is complete at the time the disc becomes too depleted for planetesimal growth. In this regard an important observable is how long stars retain their protoplanetary discs.

Observations of the near-infrared (near-IR) excess emission from stars in nearby open clusters show that the fraction of stars with

<sup>\*</sup>E-mail: wyatt@roe.ac.uk

detectable discs decreases rapidly with the age of the cluster from around >80 per cent for recently formed clusters, down to 0 per cent for 6-Myr-old clusters (Haisch, Lada & Lada 2001). Similarly no near-IR excess is found in nearby star-forming regions for stars older than 3–10 Myr (Strom et al. 1989; Kenyon & Hartmann 1995). However, a near-IR excess only implies the presence of warm dust that resides closer to the star than a few 0.1 au and it is still possible that massive outer discs exist in the older systems without material in the central au. The cool outer portions of the discs are best probed using submillimetre/millimetre observations. Such observations are particularly useful, because they also result in a reliable estimate of the disc mass. This is because the discs are transparent at these wavelengths (so all the mass is observed), and the mass estimates are relatively unaffected by uncertainties in the contribution of the stellar photosphere, as well as being only weakly dependent on estimates of the size of the dust grains and of their emitting temperature (e.g. Zuckerman 2001, see Section 6).

However, so far submillimetre/millimetre studies of the evolution of disc mass in the first 10 Myr have been inconclusive. Such observations show that while the masses of the dust discs (where present) are similar for stars of all spectral types at 30–70  $M_{\odot}$  (Mannings & Sargent 1997), it is not clear whether this disc mass does (Nünberger, Chini & Zinnecker 1997) or does not (Osterloh & Beckwith 1995) decrease with age. The evidence is also inconclusive as to whether the decay of the submillimetre disc is (Skinner, Brown & Walter 1991; Andre & Montmerle 1994; Duvert et al. 2000) or is not (Beckwith et al. 1990; Osterloh & Beckwith 1995; Nünberger et al. 1998) coincident with the disappearance of the inner disc. All studies agree, however, that by the time these stars reach the main sequence their protoplanetary discs must have been dispersed. *IRAS* showed that some 15 per cent of main-sequence stars harbour dust discs (Lagrange, Backman & Artymowicz 2000) and the very brightest of these have been detected in the submillimetre range (Zuckerman & Becklin 1993; Holland et al. 1998; Greaves et al. 1998; Sylvester, Dunkin & Barlow 2001; Sheret et al. in preparation). However, these are the only stars > 10 Myr for which discs have been detected in the submillimetre range. Also, these discs are both much less massive, typically < 0.1  $M_{\oplus}$  (Holland et al. 1998), than their younger counterparts and cannot be remnants of the protoplanetary disc, since the lifetime of this material is shorter than the age of the stars (e.g. Backman & Paresce 1993). In fact, these discs must be continually replenished, probably by the collisional breakup of asteroids or comets in the systems (Wyatt & Dent 2002) and are henceforth referred to as debris discs.

Our understanding of how a protoplanetary disc evolves into a debris disc as its host star evolves on to the main sequence has been hindered by the difficulty of finding an unbiased sample of stars of intermediate age. For late-type stars (< 2  $M_{\odot}$ ) it is well known that few such stars have been identified. Herbig (1978) noted that the T Tauri phase corresponds to just a small fraction of the pre-main-sequence lifetime of a star and inferred that a significant number of post-T Tauri stars with ages of 10–100 Myr should exist. However, such post-T Tauri stars are notoriously difficult to find, since they show few signs of youth such as active accretion and are no longer associated with regions of active star formation. The more massive (> 2  $M_{\odot}$ ) counterparts to T Tauri stars, Herbig AeBe stars, on the other hand, are found at all stages of the pre-main sequence and even up to 10 Myr after arrival on the main sequence (Waters & Waelkens 1998). Thus the evolution from protoplanetary to debris disc for higher-mass stars might occur after the star arrives on the main sequence.

One method for identifying stars of intermediate age is as the secondaries of binary systems with an O- or B-type primary (Murphy 1969; Gahm, Ahlin & Lindroos 1983), since in this case the primary must be younger than 150 Myr, and so, assuming co-evality, must the secondary. The most comprehensive list of such systems was compiled by Lindroos (1986, hereafter L86) and is comprised of 84 companions in 78 systems. This is often referred to as the *Lindroos sample*. Disc masses have been estimated for several of these Lindroos stars using submillimetre and millimetre observations (Gahm et al. 1994; Jewitt 1994; Ray et al. 1995). These studies showed no detection of dust around stars older than 10 Myr, thus supporting the hypothesis that protoplanetary discs have been depleted by this time (Jewitt 1994). However, the resulting constraints on dust mass, while below the level of T Tauri and Herbig AeBe discs, did not reach down to debris disc levels. This left open the question of whether protoplanetary discs are rapidly depleted down to, or even below debris disc levels, or whether there is a slow decline of disc mass with age (Jewitt 1994). It was the purpose of the submillimetre observations described in this paper to set limits on the dust around a subset of the Lindroos sample, approaching the level of the brightest debris discs.

A description of our subset of the Lindroos sample is given in Section 2. The submillimetre observations are described in Section 3 and in Section 4 we describe the results of these observations. In Section 5 this sample is cross-correlated with the *IRAS* data base to search for evidence of dust emission in the far-IR. In Section 6 we discuss these observations and use them to derive dust masses for this sample and discuss the implications for the evolution of protoplanetary discs. Our conclusions are given in Section 7.

## 2 SAMPLE

The Lindroos sample is comprised of 84 physical companions located 2–60 arcsec from O- and B-type primaries (L86). These were selected from the Washington Double Star catalogue (Gahm et al. 1983) and then several tests were performed to eliminate optical rather than physical associations (Lindroos 1985, hereafter L85). In this manner the sample has already been streamlined from an original list of 290 stars. The ages of the primaries, which are mostly main-sequence stars, in all of these systems were estimated from Stromgren photometry to be < 150 Myr with half of this sample being younger than 30 Myr (L85). Assuming the same age for the secondaries, which have spectral types in the range B2–K5, 37 of these must still be contracting towards the main sequence with the remainder having recently arrived there (L85).

For our sample we chose stars from Table 1 of L86 according to the following criteria. First that they have declinations  $\delta > -50^{\circ}$ . Secondly, we chose only those systems with later (> B5) type primaries. This is because the circumsecondary discs in such systems could have been affected by their interaction with the strong stellar wind and high photoionization flux of the very luminous primary star (e.g. Johnstone, Hollenbach & Bally 1998; O'Dell 2001). We also chose only systems with projected separations > 300 au. Jensen, Mathieu & Fuller (1996) used submillimetre/millimetre observations of pre-main-sequence binaries to show that disc masses are significantly lower for those systems with separations between 1 and 100 au, while the disc masses in systems with separations > 100 au are indistinguishable from those of single stars. This implies that the evolution of protoplanetary discs in systems with intermediate separation are considerably affected by the presence of a companion, presumably because of the truncation of these discs by gravitational perturbations. Our constraints allow us to

consider the evolution of the companions and of their discs as being similar to that of single stars independent of the evolution of the primary.

Finally, since the studies of Lindroos and co-authors, the physical association of some of the Lindroos sample has been tested by other authors. One of the methods used was to search for indications of youth in the secondary. Such indications include: high Li abundance (Pallavicini, Pasquini & Randich 1992; Martín, Magazzù & Rebolo 1992), detection of H $\alpha$  or Ca H and K emission (Pallavicini et al. 1992), strong X ray emission (Huélamo et al. 2000, 2001) and similar space motion to other groups of young stars (Martín et al. 1992). Another method was to check for similarity in the radial velocities of the two components (Martín et al. 1992). In rejecting erroneous Lindroos stars from our sample we took all of these studies into account, in particular omitting all pairs designated as *likely to be optical* by Pallavicini et al. (1992).

This process left us with 22 stars, which we further split into two categories according to spectral type: a group of 13 young low-mass (YLM) stars (>F0) comprising post-T Tauri (PTT) and young main-sequence (YMS) stars; and another of nine young high-mass (YHM) stars (<A9) comprising post-Herbig AeBe (PHAeBe) stars and YMS stars. The characteristics of these stars are shown in Table 1. Of the group of YLM stars, seven were identified by L85 as still contracting toward the main sequence, while they identified just one of the YHM stars (HD 47247B) as not having yet reached the main sequence. The lower fraction of pre-main-sequence stars among the higher-mass stars in this sample is inevitable given their shorter contraction time relative to the main-sequence lifetime of the B-type primaries (L85).

It should be pointed out that the studies described above to test for physical association of the Lindroos sample dealt only with potential members of our low-mass group. For this reason we should anticipate that some fraction of our YHM group could, in fact, be optical pairs (perhaps even up to 50 per cent, Pallavicini et al. 1992). Also, since this list was compiled, a study was published which compared the ages of the two components of 10 of our YLM sample based on their position in the Hertzsprung–Russell (HR) diagram relative to evolutionary tracks (Gerbaldi, Faraggiana & Balin 2001). These authors classified three of the stars in our YLM sample (HD 90972B, 108767B and 127304B) as young,  $\leq 100$  Myr, a finding corroborated by the detection of X ray emission toward these stars (Huélamo et al. 2000), but not associated with the putative primaries, since the ages they derived for the three primaries were all 200–240 Myr. Evidently there is still some uncertainty in resolving whether the Lindroos stars are physically associated as well as in determining their ages (see, e.g., Hubrig et al. 2001, for another estimate of the ages of three of our YLM primaries). In the following discussion we adopted the ages given in L86 where available.

### 3 OBSERVATIONS

The observations were made using the Submillimetre Common-User Bolometer Array, SCUBA (Holland et al. 1999) at the James Clerk Maxwell telescope (JCMT). Photometry observations were made at 850- $\mu$ m wavelength, using the central bolometer on the long-wave array. The locations of the 22 observed (secondary) stars are given in Table 1; the pointing accuracy of the JCMT is estimated to be  $\pm 2$  arcsec rms. Two of our sources were observed at 5–6 arcsec

**Table 1.** Properties of the Lindroos stars in our sample. Spectral types are taken from L86. Ages are also from L86 except for that indicated by an asterisk (HD 77484); since L86 did not provide an age estimate for this star, its age was taken from Gerbaldi et al. (2001). Distances are from *Hipparcos* except those (indicated by an asterisk) for which this was not determined with  $> 3\sigma$  uncertainty; distances to those stars were taken from L86. Projected separations are from the Washington Double Star catalogue (Worley & Douglass 1996), and the location of the secondary (or in one case tertiary) has been calculated using these offsets from the J2000 position of the primary from SIMBAD. The orbital semimajor axes ( $a$  in arcsec) of these binary systems have been estimated from their most statistically likely values based on the observed separation ( $\rho$  in arcsec):  $\log a = \log \rho + 0.13$  (Duquennoy & Mayor 1991). Objects for which excess emission is reported in the current work are shown in bold.

Primary name	Sp	Age (Myr)	Dist. (pc)	Companion name	Sp	Sep. (arcsec)	$a$ (au)	Sep. (PA)	RA (J2000)	Dec. (J2000)
(a) Low-mass companions										
HD 560	B9V	<50	100	HD 560B	G5VE	7.7	1000	160°	00 <sup>h</sup> 10 <sup>m</sup> 02.38 <sup>s</sup>	+11° 08′ 37.7″
<b>HD 1438</b>	B8V	95	212	<b>HD 1438B</b>	F3V	6.2	1800	240°	00 <sup>h</sup> 18 <sup>m</sup> 41.67 <sup>s</sup>	+43° 47′ 25.0″
HD 17543	B6IV	62	185	HD 17543C	F8V	25.2	6300	110°	02 <sup>h</sup> 49 <sup>m</sup> 19.21 <sup>s</sup>	+17° 27′ 42.9″
HD 27638	B9V	123	82	HD 27638B	G2V	19.5	2200	25°	04 <sup>h</sup> 22 <sup>m</sup> 35.55 <sup>s</sup>	+25° 38′ 03.2″
HD 33802	B8V	40	74	HD 33802B	G8V	12.7	1300	337°	05 <sup>h</sup> 12 <sup>m</sup> 17.56 <sup>s</sup>	−11° 51′ 57.5″
HD 77484	B9.5V	170(*)	250	HD 77484B	G5V	4.8	1600	92°	09 <sup>h</sup> 02 <sup>m</sup> 50.97 <sup>s</sup>	+00° 24′ 29.3″
HD 90972	B9.5V	120	147	HD 90972B	F9VE	11.0	2200	226°	10 <sup>h</sup> 29 <sup>m</sup> 34.77 <sup>s</sup>	−30° 36′ 33.0″
HD 108767	B9.5V	<112	27	HD 108767B	K2VE	24.1	880	214°	12 <sup>h</sup> 29 <sup>m</sup> 50.92 <sup>s</sup>	−16° 31′ 15.6″
<b>HD 112413</b>	A0IIIp	<28	34	<b>HD 112412</b>	F0V	19.3	890	228°	12 <sup>h</sup> 56 <sup>m</sup> 00.45 <sup>s</sup>	+38° 18′ 53.3″
HD 127304	A0V	<79	107	HD 127304B	K1V	25.8	3700	256°	14 <sup>h</sup> 29 <sup>m</sup> 47.71 <sup>s</sup>	+31° 47′ 22.1″
HD 129791	B9.5V	45	130	HD 129791B	K5V	35.3	6200	206°	14 <sup>h</sup> 45 <sup>m</sup> 56.20 <sup>s</sup>	−44° 52′ 34.8″
HD 143939	B9III	<32	168	HD 143939B	K3V	8.6	1900	217°	16 <sup>h</sup> 04 <sup>m</sup> 44.04 <sup>s</sup>	−39° 26′ 11.7″
HD 145483	B9V	<71	91	HD 145483B	F3V	3.8	470	71°	16 <sup>h</sup> 12 <sup>m</sup> 16.31 <sup>s</sup>	−28° 25′ 01.1″
(b) High-mass companions										
HD 3369	B5V	56	163(*)	HD 3369B	A6V	35.9	7900	173°	00 <sup>h</sup> 36 <sup>m</sup> 53.20 <sup>s</sup>	+33° 42′ 34.0″
HD 35173	B5V	44	331(*)	HD 35173B	B7V	26.0	12000	285°	05 <sup>h</sup> 23 <sup>m</sup> 30.00 <sup>s</sup>	+16° 02′ 32.5″
HD 47247	B5V	14	230	HD 47247B	A2V	9.1	2800	336°	06 <sup>h</sup> 36 <sup>m</sup> 40.79 <sup>s</sup>	−22° 36′ 44.7″
HD 63065	B9.5V	110	293(*)	HD 63065B	A2V	17.4	6900	9°	07 <sup>h</sup> 47 <sup>m</sup> 02.65 <sup>s</sup>	+00° 01′ 23.3″
<b>HD 74067</b>	B9V	63	86	<b>HD 74067B</b>	A2V	4.0	460	68°	08 <sup>h</sup> 40 <sup>m</sup> 19.49 <sup>s</sup>	−40° 15′ 48.4″
HD 91590	AP	38	259(*)	HD 91590B	AP	28.4	9900	162°	10 <sup>h</sup> 33 <sup>m</sup> 33.27 <sup>s</sup>	−46° 59′ 00.2″
<b>HD 99803</b>	B9Vp	126	100(*)	<b>HD 99803B</b>	A3V	13.1	1800	168°	11 <sup>h</sup> 28 <sup>m</sup> 35.33 <sup>s</sup>	−42° 40′ 39.9″
HD 159574	B8Ib	46	938(*)	HD 159574B	B7V	12.9	16000	341°	17 <sup>h</sup> 37 <sup>m</sup> 19.37 <sup>s</sup>	−40° 19′ 00.2″
HD 177817	B8IV	100	224(*)	HD 177817B	A0V	6.4	1900	2°	19 <sup>h</sup> 06 <sup>m</sup> 52.14 <sup>s</sup>	−16° 13′ 39.0″

**Table 2.** Properties of the Lindroos stars in our sample both observed and derived in this paper. All fluxes are in mJy. *IRAS* fluxes come directly from the Faint or Point Source Catalogues (FSC and PSC, respectively), apart from those indicated by an asterisk which were calculated using SCANPI (see the text for details). *IRAS* data has not been colour-corrected. Upper limits from the PSC and SCANPI are quoted at the  $3\sigma$  level, while those from the FSC are at the 90 per cent confidence level. Disc masses only include the dust mass and were calculated using equation (1); upper limits correspond to the  $3\sigma$  uncertainty and assume a dust temperature of 30 K, while the range of masses for detected discs correspond to the range of possible disc temperatures (see the text and Table 3).

Source	<i>IRAS</i>	$F_{12}$	$F_{25}$	$F_{60}$	$F_{100}$	$F_{850}$	Disc mass ( $M_{\oplus}$ )
(a) Low-mass companions							
HD 560B	F00074+1051	$278 \pm 44$	$<245$	$<130$	$<1040$	$-2.3 \pm 1.5$	$<0.5$
<b>HD 1438B</b>	F00160+4330	$128 \pm 31$	$206 \pm 27$	$413 \pm 62$	$<1370$	$-2.4 \pm 1.7$	0.05
HD 17543C	F02465+1715	$269 \pm 27$	$<137$	$<307$	$<1090$	$1.2 \pm 1.6$	$<1.8$
HD 27638B	F04195+2530	$375 \pm 45$	$<218$	$<208$	$<2010$	$0.4 \pm 1.5$	$<0.3$
HD 33802B	F05099-1155	$508 \pm 30$	$113 \pm 20$	$<242$	$<2720$	$-1.2 \pm 1.7$	$<0.5$
HD 77484B						$1.6 \pm 1.1$	$<2.3$
HD 90972B	F10273-3021	$252 \pm 30$	$<85$	$<269$	$<1660$	$0.6 \pm 1.6$	$<1.1$
HD 108767B	F12272-1614	$2560 \pm 179$	$649 \pm 71$	$<217$	$<497$	$1.0 \pm 1.5$	$<0.04$
<b>HD 112412</b>	F12536+3835	$2340 \pm 140$	$605 \pm 61$	$110 \pm 31(*)$	$<270(*)$	$3.8 \pm 1.1$	0.02–0.06
HD 127304B	F14276+3200	$153 \pm 23$	$<77$	$<210$	$<379$	$1.1 \pm 1.1$	$<0.6$
HD 129791B						$0.5 \pm 2.0$	$<1.1$
HD 143939B						$-3.3 \pm 1.9$	$<1.8$
HD 145483B	F16091-2817	$298 \pm 36$	$<184$	$<632$	$<2700$	$-0.6 \pm 2.0$	$<0.5$
(b) High-mass companions							
HD 3369B	F00341+3326	$485 \pm 34$	$<120$	$<99$	$<577$	$1.4 \pm 1.4$	$<1.2$
HD 35173B						$-3.0 \pm 1.7$	$<6.1$
HD 47247B	F06345-2234	$120 \pm 26$	$<70$	$<120$	$<742$	$-1.5 \pm 1.6$	$<2.8$
HD 63065B						$-1.1 \pm 1.4$	$<4.0$
<b>HD 74067B</b>	P08385-4005	$365 \pm 40$	$<355$	$<910(*)$	$<10600(*)$	$7.2 \pm 1.5$	0.3
HD 91590B						$-0.7 \pm 2.3$	$<5.1$
<b>HD 99803B</b>	F11261-4223	$402 \pm 36$	$<117$	$<186$	$<1370$	$4.7 \pm 1.6$	0.2–0.9
HD 159574B						$-1.3 \pm 2.9$	$<84$
HD 177817B						$1.0 \pm 1.8$	$<3.0$

from these locations, in one instance because we used coordinates for the secondary taken from SIMBAD rather than calculated from the offset from the location of the primary (HD 33802), and the other because of a coordinate transcription error (HD 127304). Since the instrumental beam size for these observations is 14.5 arcsec, we would expect to detect the flux from a point source at 60–70 per cent of its peak value; the dust masses derived from the observed fluxes given in Table 2 have been scaled accordingly. Each of our 22 sources was observed for  $2 \pm 1$  h during observing runs spread out over the period 2001 February to 2002 January.

The conventional two-position chopping and nodding technique was employed to remove the dominant sky background using a 60-arcsec chop throw in azimuth. The data were corrected for atmospheric extinction using sky opacities that were measured at the JCMT using the skydip method at appropriate intervals throughout the nights (Archibald et al. 2002). The data for each night were calibrated using Mars or Uranus when available, otherwise using the standard secondary JCMT calibrators. The data reduction was accomplished using the SURF package (Jenness & Lightfoot 1998) and anomalous signals were clipped above the  $5\sigma$  level.

SCUBA photometry observations also result in data for a further 36 bolometers on the long-wave array. The arrangement of these bolometers is such that they cover a  $\sim 2.3$ -arcmin diameter field of view, however, they are spaced so that the sky is instantaneously undersampled, thus this data cannot be used to recreate a fully sampled map. The closest of these bolometers is 21 arcsec from the target, corresponding to  $\sim 600$  au from our most nearby target. Thus we did not expect any circumstellar emission to appear in the remaining bolometers and their data were used to remove sky level variations. However, in Section 4.2 we also used these bolometers to

test for the presence of more extended emission around these stars. In this instance the bolometers were weighted according to their noise and just the outer  $\sim 70$  arcsec ring of bolometers was used for sky removal.

## 4 RESULTS OF SCUBA OBSERVATIONS

### 4.1 Photometry

The results of the observations described in Section 2 are given in Table 2. The  $1\sigma$  uncertainty achieved in these observations is  $2 \pm 1$  mJy, resulting in  $3\sigma$  upper limits of  $\sim 5$  mJy. This is an order of magnitude improvement over previous observations, which were obtained at the JCMT using the instrument UKT14 (Jewitt 1994). Submillimetre emission was detected in the central bolometer toward three stars in our sample at the  $3\sigma$  level, HD 74067B ( $7.2 \pm 1.5$  mJy), HD 112412 ( $3.8 \pm 1.1$  mJy) and HD 99803B ( $4.7 \pm 1.6$  mJy). Two of these stars are from the high-mass group, resulting in a detection rate of 22 per cent for this group, while one of the low-mass stars was detected (a detection rate of 8 per cent).

Given the high sensitivity of the observations, we might expect some detections in our sample simply from background sources such as high-redshift galaxies falling within our beam. Several estimates have been made of submillimetre number counts, the most recent being the SCUBA 8-mJy survey (Scott et al. 2002). Scott et al. estimate that there are about 620 sources  $\text{deg}^{-2}$  above 5 mJy at 850  $\mu\text{m}$  and as many as  $\sim 2000$  sources  $\text{deg}^{-2}$  should be detected above 3 mJy (Eales et al. 2000). Thus we would expect there to be one background source in any given SCUBA field of view ( $2.3 \text{ arcmin}^2$ ) at the level of  $>5$  mJy. However, only one in

100 of these sources would fall within the central photometry bolometer. Thus the probability of erroneously detecting a 5-mJy source in our sample of 22 sources is about one in five. While there is a small (20 per cent) chance that one of our detections is, in fact, of a background source, it is very unlikely that all three submillimetre sources are unassociated with the programme stars.

With such a high sensitivity it is also necessary to check whether we might (or indeed should) have detected the photospheric emission of any of the stars. However, even the two closest primaries (HD 108767 and 112413) have predicted photospheric fluxes of  $<0.6$  mJy at  $850\ \mu\text{m}$ . The more distant primaries, as well as all the secondaries, have predicted fluxes much less than this.

Another consideration for our observations given the large beam size is that for several of our sources the primary falls within the beam when pointing at the companion (e.g. if their separation is less than about 7–8 arcsec, see Table 1). In such cases any emission that is detected could originate near the primary and not the secondary star. Consider the HR4796 wide binary system, which hosts a circumprimary disc, but not a circumsecondary disc (Jayawardhana et al. 1998). At 7.7-arcsec separation a SCUBA  $850\text{-}\mu\text{m}$  observation centred on the companion would have detected  $\sim 46$  per cent of the emission from the circumprimary disc (i.e.  $\sim 9$  mJy, Greaves, Mannings & Holland 2000). This uncertainty is relevant for our detection of emission toward HD 74067B, since this star is just 4 arcsec from HD 74067A. If the emission we detected for HD 74067B is actually centred on the primary (and point-like), it would have been underestimated in Table 2 by 80 per cent. The emission detected in the vicinity of HD 112412 and 99803B, however, could not have its origin near the primary stars in these systems, since at 19.3- and 13.1-arcsec offset, these lie outside the beam.

#### 4.2 Search for extended emission

In general, any emission from circumstellar discs in the systems we observed should come from within a few arcsec of the stars, assuming these discs have a typical size of less than a few hundred au, and so should lie within the central bolometer. However, in the case of HD 74067 we were inspired to search for emission from the region around this system because it is in the galactic plane (galactic latitude  $b = 0:52$ ) with extended cirrus emission nearby (though not peaked on this system) evident from the *IRAS*  $100\text{-}\mu\text{m}$  image. It was thus questionable as to whether the detection is of a circumstellar disc, cirrus heated by the stars or indeed the chance alignment of a background or foreground cirrus hotspot. One test is to see whether the emission is extended on greater than arcmin scales, since this is a characteristic of other cirrus hotspots detected both in the far-IR from its thermal emission (Gaustad & Van Buren 1993) and in the optical range as reflection nebulae (Kalas et al. 2002).

Thus we repeated the data reduction using the outer ring of 18 bolometers at 62–82 arcsec from the centre of the array to estimate the sky level. We then looked at the mean flux levels in the rings of six and 12 bolometers at 21–28 and 40–55 arcsec from the centre, respectively; this part of the reduction was done using IDL. Significant emission was indeed detected in both rings, decreasing from an average  $\text{mJy beam}^{-1}$  of  $6.7 \pm 1.4$  at the centre<sup>1</sup> to  $2.5 \pm 0.6$  at

<sup>1</sup> The average  $\text{mJy beam}^{-1}$  at the centre is a factor of 1.075 lower than the mJy derived by reducing photometry observations (which is the figure given in Table 1), since during such observations the central bolometer performs a 4 arcsec<sup>2</sup> nine-point jiggle pattern about the centre (Holland et al. 1999). Reduction of photometry accounts for this to find the flux at the centre assuming we are observing a point source.

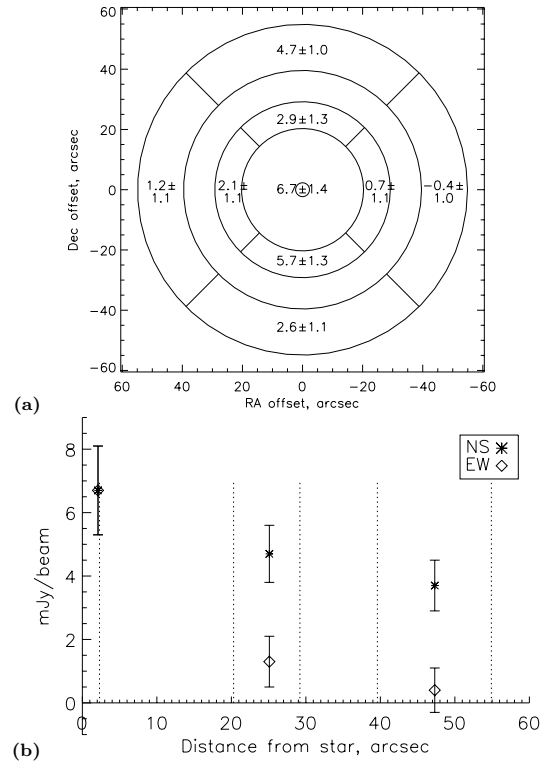


**Figure 1.** The distribution of the  $850\text{-}\mu\text{m}$  emission detected around HD 74067B: (a) undersampled map. The circles show the extent of the first and second rings of bolometers at 21–28 and 40–55 arcsec, respectively. These rings have been subdivided into quadrants and the mean (and its error) of the data points falling into each quadrant are shown in units of the average mJy beam<sup>-1</sup> in this region. (b) Radial distribution of emission. Each data point corresponds to the average of all data with a position angle within  $90^\circ$  of N or S (asterisk symbol) and E or W (diamond symbol).

25 arcsec and  $1.9 \pm 0.5$  at 47 arcsec from the star. The outer ring at 70 arcsec showed no emission ( $0.3 \pm 0.4$  mJy beam<sup>-1</sup>) as expected as this was used to estimate the sky level.

We also checked to see whether this emission is symmetrically distributed around the star. To do this we put individual data points into different bins according to their radial distance from the star and position angle on the sky and then obtained the mean and standard deviation in each bin with the different bolometers of different observations weighted according to their noise. In this way we split each bolometer ring into four quadrants. The findings are summarized in Fig. 1. The emission does appear to be asymmetrical in that the only significant emission component is in the N and S directions for both bolometer rings. Combining the data for diametrically opposite quadrants we find that the average mJy beam<sup>-1</sup> in the N+S direction at 25 and 47 arcsec is  $4.2 \pm 0.9$  and  $3.7 \pm 0.8$ , respectively, while that in the E+W direction is just  $1.3 \pm 0.8$  and  $0.4 \pm 0.7$  at the same distances. We changed the position angle of the quadrant pattern in Fig. 1 to maximize the asymmetry and estimate the error on this angle to be  $0^\circ \pm 30^\circ$ . An asymmetry is also apparent in the bolometer ring at 70 arcsec, with an average mJy beam<sup>-1</sup> of  $1.5 \pm 0.6$  in the NE+SW direction compared with  $-1.3 \pm 0.6$  NW+SE. This indicates that the emission could extend to 70 arcsec from the star. If so, since the mean flux in this bolometer ring was used to subtract the sky emission from the remaining bolometers, the sky

level would have been overestimated and the fluxes given in Fig. 1 are too low by  $\sim 1.3 \text{ mJy beam}^{-1}$ .

While it is possible that the asymmetry is caused by real structure in the emitting material, the signals measured are also consistent with a symmetrical centrally peaked structure extending to  $\sim 70 \text{ arcsec}$  from the stars. In such an interpretation, the asymmetry arises because some of the symmetrical emission has been artificially eliminated by chopping just  $60 \text{ arcsec}$  on to the same structure. Because the observations were all undertaken just before or just after transit, the position angle of the azimuth chop was within  $\pm 40^\circ$  of E–W for all of our observations. Thus if the emission is centrally peaked, our E+W observations should be lower than those N+S. Assuming the observed N+S emission in Fig. 1(b) is the level at which E+W emission should have been observed if chopping off-source, chopping on-source would have resulted in E+W fluxes  $\sim 3 \text{ mJy beam}^{-1}$  lower than those in the N+S direction in both rings of bolometers, consistent with that observed; the emission in the central bolometer would also have been underestimated by a similar amount. To test whether the structure is dependent on the chop position angle, we split the data set into that taken before and after transit, with chop position angles of  $72^\circ \pm 7^\circ$  and  $126^\circ \pm 6^\circ$ , respectively. The position angle of the structure derived was indeed found to be higher for the post-transit observations by  $\sim 45^\circ$  for all rings of bolometers. We conclude that this emission extends to  $70 \text{ arcsec}$  from the star, is centrally peaked and that a significant component is symmetrically distributed around the star.

This process was now repeated for the other stars for which emission was detected. No significant extended emission was detected in the vicinity of either HD 99803B or HD 1438B. However, additional emission was detected in the bolometer ring  $25 \text{ arcsec}$  from HD 112412, where the average  $\text{mJy beam}^{-1}$  is  $2.0 \pm 0.4$ . Averaging the data points lying within  $7.3 \text{ arcsec}$  (i.e. within one beam) of different points close to and within this ring showed that this emission can be resolved into three distinct sources (see Fig. 2) with no significant emission detected in the remainder of the ring. (i) The first source appears to be centred  $\sim 4 \text{ arcsec}$  N of the primary HD 112413 (i.e. at  $14 \text{ arcsec}$  E and  $17 \text{ arcsec}$  N of HD 112412) with a flux of  $5.5 \pm 1.6 \text{ mJy}$ . Since this source is undersampled, we estimate the

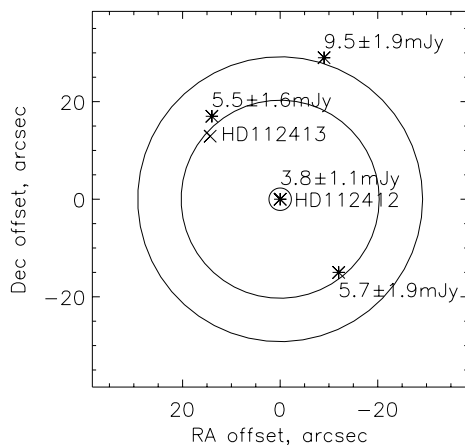


**Figure 2.** The distribution of the  $850\text{-}\mu\text{m}$  emission detected around HD 112412. The circles show the extent of the first ring of bolometers at  $21\text{--}28 \text{ arcsec}$ . The circumsecondary disc located at the centre of the map and the three additional sources detected in the first bolometer ring are shown by asterisks and their flux level is also given. The location of HD 112413 is shown with a cross.

uncertainty in its position be  $\pm 5 \text{ arcsec}$  and we attribute this emission to a circumprimary disc; this undersampling also means that the absolute level of the emission is not well constrained, with an additional uncertainty estimated to be  $\sim 30 \text{ per cent}$ . (ii) Another source is located  $9 \text{ arcsec}$  W and  $29 \text{ arcsec}$  N of HD 112412 with a flux of  $9.5 \pm 1.9 \text{ mJy}$  (with similar uncertainties in these values). (iii) A third source is detected almost diametrically opposite HD 112413 at a location of  $12 \text{ arcsec}$  W and  $15 \text{ arcsec}$  S of HD 112412 with a flux of  $5.7 \pm 1.9 \text{ mJy}$ . We note that we would not be able to tell whether the emission detected toward HD 112412, 112413 and source (iii) forms part of an extended structure, since the regions between the sources were not sampled (see, e.g., Fig. 2).

As a result of the high proportion of detections we found using this method (2/4), it was questioned whether the non-standard reduction procedure was producing false results. We looked for emission near all the remaining stars in our sample. The only detection was of emission of  $7.4 \pm 2.1 \text{ mJy}$  located  $42 \text{ arcsec}$  E and  $31 \text{ arcsec}$  S of HD 145483B. In the absence of fully sampled maps it is not possible to determine the true nature of the offset sources (ii) and (iii) near HD 112412 and of the source near HD 145483B. However, as the two additional bolometer rings we checked cover a  $\sim 5000 \text{ arcsec}^2$  field of view, we would expect to detect  $\sim 5$  unrelated background sources in our sample of 22 stars at the  $\geq 5 \text{ mJy}$  level (see Section 4.1), thus we do not discuss these detections further in this paper.

## 5 CROSS-CORRELATION WITH *IRAS*

Also shown in Table 2 is a cross-correlation of our sample with the *IRAS* Faint Source and Point Source Catalogues (hereafter FSC and PSC, respectively). These catalogues provide flux densities measured in four wavelength bands centred at  $12$ ,  $25$ ,  $60$  and  $100 \mu\text{m}$ , and were searched for sources within  $60 \text{ arcsec}$  of our programme stars. In this way emission was detected toward  $14/22$  of our programme stars. Since the FSC is  $\sim 2.5$  times more sensitive than the PSC, these results are shown preferentially. Just one of our detections (HD 74067B) did not turn up in the FSC, and this is because the FSC excludes sources within  $10^\circ$  of the galactic plane (i.e. those with  $|b| < 10^\circ$ ).

For all of these detections, the  $12\text{-}\mu\text{m}$  flux is consistent with that expected from the photospheres of the primary stars in these systems by extrapolating their  $K$ - (where available in the literature or from the 2MASS data base) or  $V$ -band magnitudes. The photospheres of the three closest stars (HD 108767, 112413 and 33802) were also detected at  $25 \mu\text{m}$ . For one of the stars, HD 1438, excess emission was detected above photospheric levels at both  $25$  and  $60 \mu\text{m}$  at  $185 \pm 31$  and  $409 \pm 62 \text{ mJy}$ , respectively.<sup>2</sup> The positional uncertainty of the *IRAS* source is such that we cannot distinguish whether this emission originates nearer the primary or secondary component in this system. This uncertainty is particularly pertinent when we consider that a system which just missed inclusion in Lindroos' list because the primary is a main-sequence A0 star, HR4796, shows evidence from mid-IR imaging of a dust disc around the primary but not one around the pre-main-sequence M-type secondary (Jayawardhana et al. 1998). At  $7.7\text{-arcsec}$  separation, it had not previously been possible to tell which star hosted the far-IR emission detected by *IRAS*. We suggest that subsequent mid-IR imaging of this system would resolve this issue.

<sup>2</sup>The colour-corrected photospheric emission has been subtracted from these fluxes, but no colour correction was applied to this excess.

A similar cross-correlation of the Lindroos sample with the *IRAS* catalogues was performed by Ray et al. (1995) and included 10 of our low-mass sample. These authors reported the detection of non-photospheric emission towards seven of these sources in all four wavebands. It appears that they interpreted all fluxes reported in the *IRAS* catalogues as positive detections, whereas the correct interpretation of a flux reported with FQUAL = 1 is that it is an upper limit ( $3\sigma$  for the PSC, 90 per cent confidence for the FSC) as reported in this paper.

Even greater sensitivity can be obtained from the *IRAS* data base using SCANPI (*IRAS* Scan Processing and Integration), available at the Infrared Science Archive (IRSA) website (<http://irsa.ipac.caltech.edu>). This performs averaging of the *IRAS* raw survey data scans passing close to a given location. We used this to coadd the scans near our survey sources. This resulted in better ( $3\sigma$ ) upper limits to the far-IR fluxes at the location of some of our submillimetre detections, as well as the detection of the photosphere of HD 112413 at 60  $\mu\text{m}$ . Also, emission was detected centred on HD 17543C in the in-scan direction ( $342^\circ$  position angle) at 60  $\mu\text{m}$  with a peak of  $220 \pm 23$  mJy. However, this emission appears extended in the cross-scan direction, since a similar level of emission appears in scans taken up to 2 arcmin from the star. Indeed, there is a 60- $\mu\text{m}$ -only source of  $247 \pm 42$  mJy in the FSC, F02464+1714, located 106 arcsec from HD 17543C at a position angle of  $254^\circ$ . We attribute this source either to local cirrus cloud heated by the stars or to an unrelated object and do not discuss it further in this paper.

## 6 DISCUSSION

### 6.1 SED modelling and dust masses

While it is clearly unrealistic to model the spectral energy distributions (SEDs) of the infrared excesses of these stars using just one or two data points, the upper limits obtained at different wavelengths can set useful constraints on the temperature of the emitting dust. These can then be used to check whether the spatial extent of the emission is consistent with that observed and to compare the sensitivities of the *IRAS* and SCUBA to the types of dust emission that were detected.

The SED is modelled here assuming what is sometimes referred to as *modified blackbody* emission. The dust is assumed to emit at a single temperature,  $T$ , and its emission efficiency  $Q_v$  is assumed to be unity (i.e. to emit like a blackbody) below a critical wavelength,  $\lambda_0$ , and to fall off  $\propto \lambda^{-\beta}$  at longer wavelengths. Comparison with the observed and predicted emission properties of real grains shows that  $\lambda_0 \approx a$ , the typical size of the dust grains, and that  $\beta$  lies in the range 0.5–2 (Bohren & Huffman 1983; Pollack et al. 1994). Interstellar extinction curves show that interstellar-type grains have  $\beta \approx 2$  (e.g. Mathis 1990). Modelling of the observed SEDs of young stellar objects (YSOs), T Tauri discs and debris discs around main-sequence stars shows that at the early stages of the evolution of a disc  $\beta \approx 1.5$ , while for more evolved discs  $\beta = 0.5$ –1 (Dent, Matthews & Ward-Thompson 1998; Dent et al. 2000). Thus, given the age of our sample, we expect their disc emission to be fitted by grains with  $\beta$  close to 1. In the following discussion we set  $\beta = 1$  and  $\lambda_0 = 100$   $\mu\text{m}$ , and for comparison also show model fits for  $\beta = 0$  and 2. The results of the modelling for each star are discussed below (see also Fig. 3 and Table 3).

Dust masses were estimated from the observed submillimetre flux, since these give a reliable estimate of the dust mass of a disc (Zuckerman 2001), although for the far-IR-only detection we used the 60- $\mu\text{m}$  flux. The appropriate formula is (e.g. Zuckerman &

Becklin 1993; Zuckerman 2001)

$$M_{\text{dust}} = \frac{F_v D^2}{\kappa_v B_v(T)}, \quad (1)$$

where  $F_v$  is the observed flux,  $D$  is the distance to the star,  $\kappa_v = 0.75 Q_v / a \rho$  is the dust opacity at the observed wavelength ( $\rho$  is the dust density) and  $B_v$  is the blackbody intensity at the dust temperature. For consistency with the masses derived by other authors (e.g. Zuckerman & Becklin 1993; Greaves et al. 1998; Holland et al. 1998; Sylvester et al. 2001) we adopted a dust opacity of  $0.17 \text{ m}^2 \text{ kg}^{-1}$  at 850  $\mu\text{m}$  and scaled to 60  $\mu\text{m}$  assuming  $\beta = 1$  (giving an opacity of  $2.4 \text{ m}^2 \text{ kg}^{-1}$ ). For dust temperatures of 30–100 K, observed fluxes at 850  $\mu\text{m}$  correspond to  $11$ – $2.7 \times 10^{-3} D^2 F_v$  Earth masses, where  $D$  is in parsec; dust masses derived from 60- $\mu\text{m}$  fluxes are much more dependent on the assumed temperature of the dust. The derived dust masses for our sample are reported in Table 2.

#### 6.1.1 HD 1438B

Since the excess emission is detected at two wavelengths we can derive its temperature to be  $\sim 107$  K. The modified blackbody fit is shown by the dashed line in Fig. 3(a). This temperature implies a distance of either 10 au from HD 1438B or 90 au from HD 1438 if the dust emits as a blackbody. These distances would be larger if the grains are small and so emit hotter than black bodies at an equivalent distance (Wyatt et al. 1999). Thus if this emission is circumprimary, it should be possible to resolve this disc in the mid-IR from an 8-m class telescope.

It is not surprising that this disc was not detected in the submillimetre range, since the fit with  $\beta = 1.0$  predicts  $F_{850} = 0.8$  mJy. In fact, our upper limit of 5.1 mJy at 850  $\mu\text{m}$  only rules out that the grains emit as perfect black bodies with  $\beta < 0.1$ . The upper limit to the dust mass derived from the submillimetre flux is  $0.6 M_\oplus$ , while the 60- $\mu\text{m}$  flux implies that we have detected material with a mass of just  $\sim 0.05 M_\oplus$ . This is similar to the mass of the debris discs found around young main-sequence stars such as  $\beta$  Pictoris (e.g. Holland et al. 1998). We have also determined the fractional luminosity of the dust disc with respect to that of the star,  $f = L_{\text{ir}} / L_\star$ . If this is a circumprimary disc  $f \approx 0.3 \times 10^{-3}$ , a value typical of other debris discs, whereas if circumsecondary  $f \approx 0.01$ , which would make it one of the most luminous debris discs.

#### 6.1.2 HD 74067B

Consider first of all the submillimetre emission detected in the central bolometer. Fig. 3(b) shows fits scaled to the 850- $\mu\text{m}$  flux assuming  $\beta = 0.0, 1.0, 2.0$  (dash-dot, dashed and dotted lines, respectively). These grain properties and the constraints from the *IRAS* non-detections imply dust temperatures of less than 120, 56 and 34 K, and dust masses of at least 0.1, 0.3 and  $0.5 M_\oplus$ , respectively. It is possible to rule out interstellar-type ( $\beta = 2.0$ ) grains as the origin of this emission, since such grains must lie within 7.3 arcsec of HD 74067B and, given the 4-arcsec projected separation of this binary system, are also likely to be within 1000 au of HD 74067. Such grains emit hotter than black bodies since they absorb stellar radiation more efficiently than they re-radiate it at longer wavelengths. The emission efficiencies of interstellar-type grains imply that they would be heated to  $\sim 110$  K at 1000 au from HD 74067 (compared with a blackbody temperature of  $\sim 27$  K). Since the observed grains are relatively cool for their distance from the primary star (given the *IRAS* limits), we infer that they must have  $\beta < 1.0$ , although the exact value depends on the assumed value of  $\lambda_0$ .

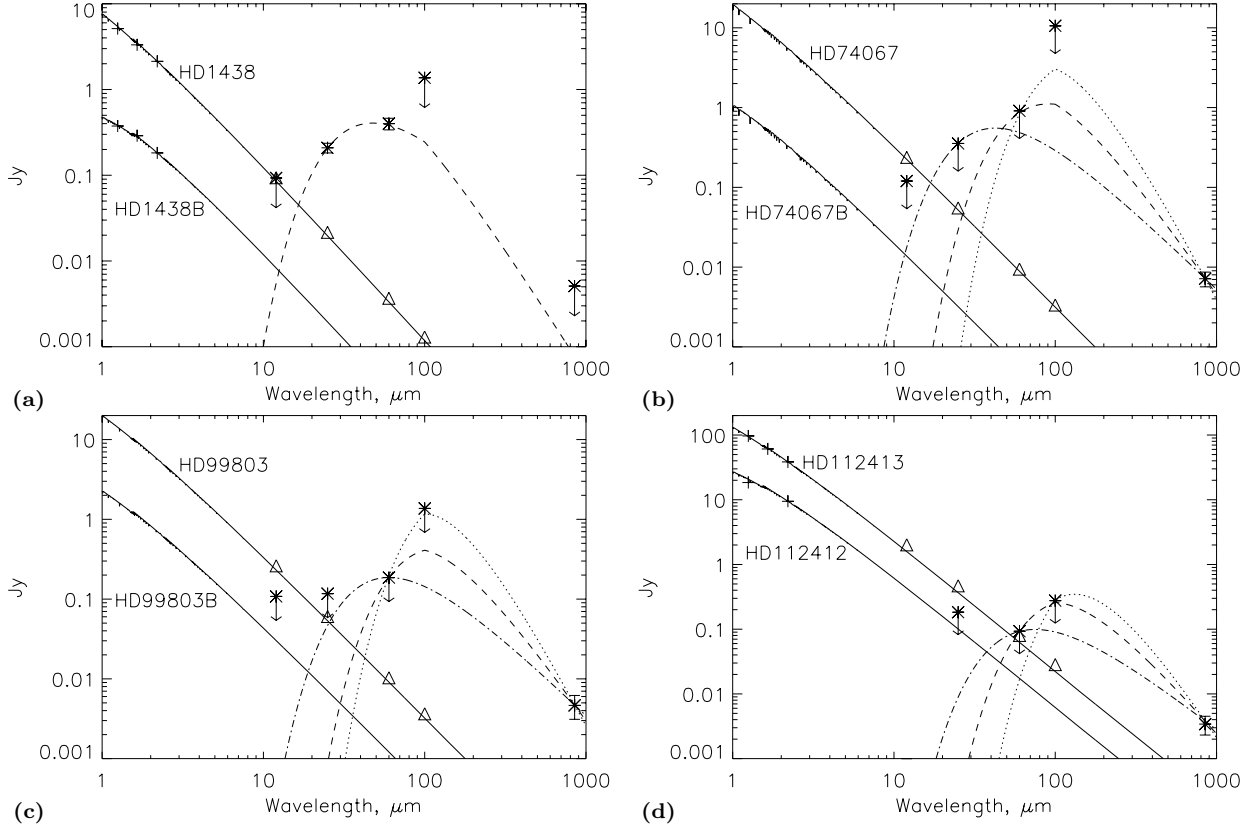


**Figure 3.** Spectral energy distributions of the emission towards the four stars for which excess emission is reported in this paper: (a) HD 1438B, (b) HD 74067B, (c) HD 99803B and (d) HD 112412. Stellar spectra were determined from Kurucz model atmospheres appropriate to the spectral type, and were scaled to the  $K$  magnitude (or  $V$  magnitude if unavailable) which are plotted with plus symbols. The *IRAS* and SCUBA fluxes are plotted with asterisks. Since the *IRAS* fluxes given in Table 2 include a contribution from the photospheric emission of both stars in the system (shown with triangular symbols), this has been colour-corrected and subtracted before plotting. In the case of HD 1438, the resulting fluxes have been further colour-corrected for a 107-K blackbody. The dashed and dotted lines show modified blackbody fits to the excess emission and are discussed in the text; note however that the fits in (b), (c) and (d) are constrained by the *IRAS* upper limits and the actual far-IR emission could fall below this level.

**Table 3.** Results of SED modelling for the emission detected towards HD 1438B, 74067B, 99803B and 112412 (see Fig. 3). Here we give the derived dust temperature  $T$ , the distance from the secondary star  $r_B$  of blackbody grains emitting at this temperature, and the corresponding mass of the  $M_{\text{dust}}$  for different assumed dust properties defined by the parameter  $\beta$ . The appropriate lines on Fig. 3 for these models are also given.

Source	$\beta$	$T$ (K)	$r_B$ (au)	$M_{\text{dust}}$ ( $M_{\oplus}$ )	Fig. 3
HD 1438B	$>0.1$	107	10 (or $r_A = 90$ au)	0.05	Dashed
HD 74067B	0.0	$<120$	$>30$	$>0.1$	Dash-dot
	1.0	$<56$	$>130$	$>0.3$	Dashed
	2.0	$<34$	$>340$	$>0.5$	Dotted
HD 99803B	0.0	$<85$	$>50$	$>0.2$	Dash-dot
	1.0	$<42$	$>200$	$>0.3$	Dashed
	2.0	$<29$	$>420$	$>0.5$	Dotted
		$>20$	Heating by primary	$<0.9$	
HD 112412	0.0	$<68$	$>40$	$>0.02$	Dash-dot
	1.0	$<38$	$>140$	$>0.04$	Dashed
	2.0	$<22$	$>410$	–	Dotted
		$>25$	Heating by primary	$<0.06$	

While the distribution and level of the emission detected  $>25$  arcsec from the star remains uncertain due to the nature of our observing method, the fact that this emission was detected implies a substantial mass of dust. If the emission is symmetrically distributed

about the stars with a level of 4.2 and 3.7 mJy beam $^{-1}$  at 25 and 47 arcsec, this implies integrated fluxes of 45 and 75 mJy in rings of one beamwidth at these distances. Further assuming emission at blackbody temperatures (19 and 14 K, respectively, based on the projected separations from HD 74067), this implies dust masses of 7 and 20  $M_{\oplus}$ , with more mass expected to have remained unobserved between the bolometer rings.

Similar arguments to those in the paragraph above argue against the presence of interstellar-type grains, since these would be heated to 84 and 66 K at 2200 and 4000 au from HD 74067. However, we note that the interaction of the stars with an interstellar dust cloud would mean that only the largest grains from that cloud could penetrate close to the stars, since the smaller (few 0.1- $\mu\text{m}$ ) grains that dominate the interstellar extinction curves would be repelled by radiation pressure (Artymowicz & Clampin 1997). Thus the cool temperature of the excess emission could not on its own rule out the interaction of the stars with a cirrus cloud as the cause of this excess. However, the mean Galactic density of solid grains is just  $\sim 7 \times 10^{-15} M_{\oplus} \text{ au}^{-3}$  (Artymowicz & Clampin 1997). Thus, as we infer a mass density from our submillimetre observations of at least  $7 \times 10^{-11} M_{\oplus} \text{ au}^{-3}$ , then if this dust is interstellar in origin, the star must be in a region of the galaxy with at least 10 000 times the mean Galactic density. This is unlikely, since at  $\sim 60$  Myr this system should not still reside in the cloud from which it was born,



and such a high density would only apply in molecular clouds which fill just 0.2 per cent of the Galactic stellar disc.

We conclude that the material at  $>25$  arcsec must be either bound to HD 74067 (e.g. in a massive  $>27 M_{\oplus}$  extended  $\sim 6000$ -au circumbinary disc or remnant protostellar envelope) or an unrelated background object (e.g. a nearby galaxy or Galactic cloud). This system is unusual in our sample for two reasons that argue in favour of the different interpretations: the orbital semimajor axis of this pair (460 au, Table 1) is the smallest in the sample, thus increasing the chances of survival of a circumbinary disc; and this is the only system in the galactic plane, thus increasing the chance of alignment with a background object. Further observations of this region are required to determine the origin of this emission.

We note that extended circumbinary envelopes have been proposed as the replenishment mechanism of T Tauri discs in binary systems (Prato & Simon 1997), a proposal which may be supported by interferometric observations of binary T Tauri systems that detect a lower level of emission than single-dish measurements, possibly implying the presence of additional extended emission (Jensen & Akeson 2003). Also, if this material is circumbinary, then the orbital semimajor axis of the binary (460 au, Table 1) implies that any circumbinary disc would be truncated within  $\sim 9$  arcsec of a point roughly midway between the two stars (see Table 1 of Artymowicz & Lubow 1994). Thus, if this is the case, the emission detected in the central bolometer would have to be circumstellar, not circumbinary, in origin, and further would be truncated at  $\sim 150$  au (1.7 arcsec) from either star (see Table 1 of Papaloizou & Pringle 1977), again ruling out the models with  $\beta > 1.0$  (see Table 3).

### 6.1.3 HD 99803B

The SED fit was scaled to the observed  $850\text{-}\mu\text{m}$  flux, and upper limits to the temperature of the dust emission calculated for different  $\beta$ . For  $\beta = 1.0$ , shown with the dashed line in Fig. 3(c), this temperature must be below 42 K to avoid contradiction with the non-detection by *IRAS*. This corresponds to dust at least 200 au (2 arcsec) from HD 99803B, while the inferred orbital semimajor axis of this system (1800 au, Table 1) implies that any circumbinary disc should be truncated beyond 540 au from HD 99803B (Papaloizou & Pringle 1977). This model implies a dust mass of at least  $0.3 M_{\oplus}$  and a fractional luminosity of  $0.6 \times 10^{-3}$ .

Models with  $\beta = 0.0$  and  $2.0$  are also shown in Fig. 3(c) with dash-dot and dotted lines, respectively. These imply that if the dust emits as a blackbody, its temperature could be as high as 85 K (dust as close as 50 au with a mass of  $0.2 M_{\oplus}$ ). Interstellar-type dust with  $\beta = 2.0$ , however, require that  $T < 29$  K (dust as close as 420 au with a mass of  $0.5 M_{\oplus}$ ). Dust orbiting HD 99803B would be heated to  $>20$  K by the 1800-au distant primary star giving an upper limit to the dust mass of  $0.9 M_{\oplus}$ .

### 6.1.4 HD 112412 and 112413

Starting with HD 112412, the SED model was scaled to the observed  $850\text{-}\mu\text{m}$  flux, from which upper limits to the temperature of the dust emission were calculated for different  $\beta$ . For  $\beta = 1.0$ , shown with the dashed line in Fig. 3(d), this temperature must be below 38 K to avoid contradiction with the non-detection by *IRAS*. This corresponds to dust at least 140 au (4 arcsec) from HD 112412 and implies a dust mass of at least  $0.04 M_{\oplus}$  and a fractional luminosity of  $4 \times 10^{-5}$ . Since the emission falls within the beam, we also know that the emission arises  $<250$  au from HD 112412. This is consistent with

the expected truncation radius of the circumsecondary disc due to its tidal interaction with the primary at 260 au (Papaloizou & Pringle 1977).

Models with  $\beta = 0.0$  and  $2.0$  are also shown in Fig. 3(d) with dash-dot and dotted lines, respectively. These imply that if the dust emits as a blackbody, its temperature could be as high as 68 K (dust as close as 40 au with a mass of  $0.02 M_{\oplus}$ ). The dust cannot, however, have  $\beta = 2.0$ , as such models require that  $T < 22$  K and so that the dust is further than 410 au from HD 112412; this constraint is incompatible with the emission falling within the beam. In fact, both the temperature and distance constraints are also inconsistent with the implied distance to the primary star of 890 au (Table 1), since this would both truncate the circumsecondary disc (see above) and heat dust falling in the beam centred on HD 112412 to  $>25$  K. This 25 K lower limit to the circumsecondary dust temperature also means that its dust mass is unlikely to be more than  $0.06 M_{\oplus}$ .

Since the *IRAS* upper limits also apply to the emission from the disc around HD 112413, and the circumprimary  $850\text{-}\mu\text{m}$  emission is the same (within the uncertainty) as that from the circumsecondary disc (see Section 4.2), the temperatures and masses derived from the SED models in Fig. 3(d) (see Table 3) are also valid for the circumprimary disc. The factor of  $\sim 8$  times higher luminosity of an A0III to an F0V star, however, means that the limits from these models to the distance of the dust from HD 112413 should be approximately 2.8 times the value of  $r_B$  given in Table 3. Thus, since for this emission to fall within the beam it must be  $<250$  au from the star, we can rule out models with  $\beta$  greater than about 0.5; i.e. to account for the *IRAS* non-detections, the circumprimary grains must emit very much like black bodies at temperatures of  $<49$  K.

## 6.2 Detection summary

Of the 22 stars in our sample, we detected the following.

- (i) One warm (100–110 K) circumstellar disc toward HD 1438 with *IRAS*, but not with SCUBA; it was not possible to tell whether this is circumprimary or circumsecondary.
- (ii) One system, HD 74067, with centrally peaked extended emission, possibly indicating the presence of a nearly face-on circumbinary disc/envelope extending to  $\sim 6000$  au, and an additional circumstellar component.
- (iii) Two cold ( $<40$  K assuming  $\beta = 1$ ) circumsecondary discs around HD 112412 and 99803B in the submillimetre range with SCUBA, but not in the far-IR with *IRAS*; the SCUBA observations also showed that one of these systems hosts a cold ( $<50$  K assuming  $\beta = 0.5$ ) circumprimary disc (around HD 112413).

A quick look at Table 1 shows that, at least within this sample, there is nothing unusual about those systems with circumstellar discs in terms of their age or binarity, since the detected systems span the range of binary separation and age. There does, however, appear to be a correlation with spectral type, since all detections were around stars earlier than F3 ( $>3 L_{\odot}$ ); none of the eight solar-like G or K stars were found to harbour discs. There is also a correlation with distance in that the two detections in the YHM group were of the closest stars of that group, and that in the YLM group was of the second closest. This leaves the possibility open that all stars in the YHM group and the majority of stars in the YLM group have cold discs that are similar in mass to those detected around HD 99803B and 112412 (see Fig. 4).

It is unusual that the circumprimary HD 112413 disc is not much more massive than the circumsecondary HD 112412 disc, since near-IR and millimetre observations of binary systems in Taurus-Aurigae

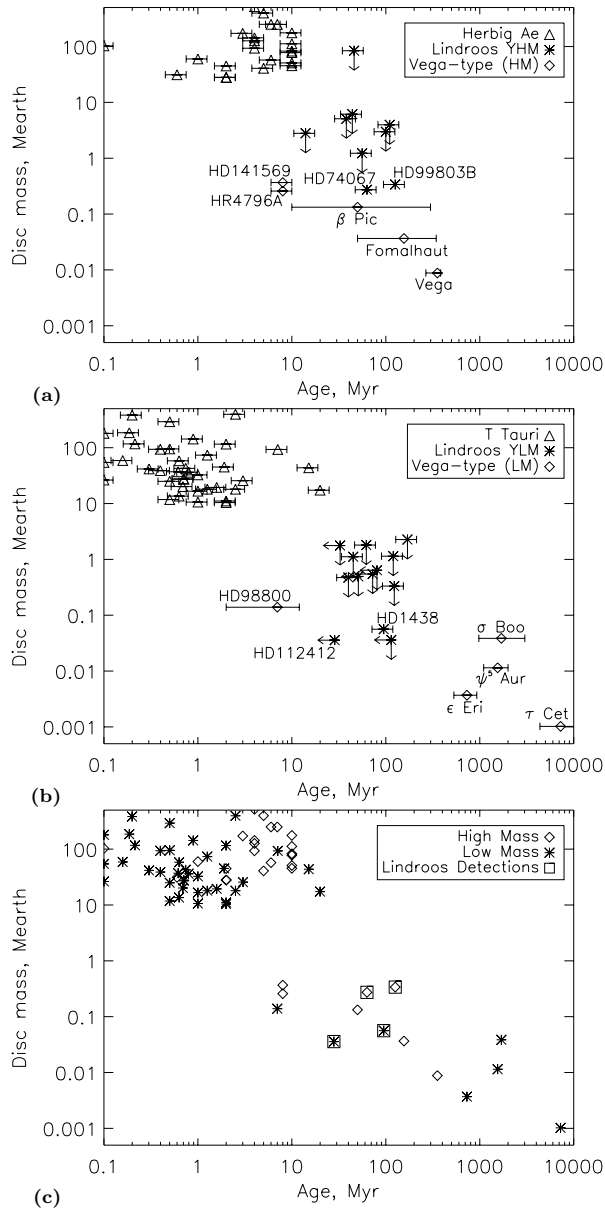


**Figure 4.** The evolution of dust mass for low-mass (a) and high-mass (b) stars. For all stars plotted, dust masses were calculated using equation (1) and published submillimetre or millimetre fluxes as well as estimates of the dust temperature and system distance. As well as the results of this study, we also show detections of T Tauri discs (Jewitt 1994; Osterloh & Beckwith 1995; Nürnberg et al. 1997, 1998) and of Herbig AeBe discs (Mannings & Sargent 1997; and lists compiled by Natta et al. 1997 and Meeus et al. 2001); the errors in the ages are nominally plotted at  $\pm 25$  per cent. Also plotted are the Vega-type stars for which submillimetre observations have confirmed the *IRAS* excess to originate in a circumstellar disc (Holland et al. 1998; Greaves et al. 1998; Sylvester et al. 2001; papers by Wyatt, Greaves, Sheret et al. in preparation), and for which ages, with appropriate errors, are available in the literature (Lachaume et al. 1999; Song et al. 2000, 2001). The bottom figure (c) combines the results shown in (a) and (b), and for clarity omits the Lindroos non-detections and the error in the ages.

show that circumsecondary discs, if present, are much less massive than circumprimary discs (White & Ghez 2001; Jensen & Akeson 2003). A more massive circumprimary disc is also expected from theoretical predictions of binary star formation (Bate & Bonnell 1997), and is certainly true of the quasi-Lindroos system HR4796 (Jayawardhana et al. 1998). However, since HD 112413 is the only system in our sample for which information was obtained about its circumprimary emission, we cannot draw any conclusions on this subject.

### 6.3 Submillimetre disc population

What is particularly striking about these results is that 9–14 per cent of this sample (two or three out of 22) have discs that were not detected by *IRAS*. This fraction is even higher at 20–30 per cent (two or three out of 10) if we consider just stars more massive than  $1.5 M_{\odot}$  ( $< F0$ ), and even higher still (up to 4/11) if we include the circumprimary disc detected around HD 112413. To the best of our knowledge, just one circumstellar disc, that around the M1 star TWA7 (Zuckerman 2001), has been discovered around an isolated star that was not detected first in the far-IR by a space-based telescope such as *IRAS* or *ISO*. The majority of searches for discs in the submillimetre range have been directed toward stars for which excess emission is already known in the far-IR. However, such searches are biased toward relatively warm discs. The fact that SCUBA was able to detect these discs while *IRAS* could not must be because these discs are cold ( $< 40$  K if  $\beta = 1$ ; Section 6.1). Thus these results imply that a significant population of cold submillimetre discs could be awaiting discovery in more unbiased submillimetre surveys, a finding which is supported by the fact that the TWA7 disc was discovered in a submillimetre survey of the TW Hydrae Association (Zuckerman et al., in preparation), members of which do not necessarily have *IRAS* excesses. Depending on their temperature, these cold discs could also be detected by deep far-IR observations using, for example, *SIRTF* or *SOFIA*, and indeed such observations in conjunction with those in the submillimetre are required to determine the temperature of these discs.<sup>3</sup>

Since current estimates put the fraction of main-sequence stars with discs at 15 per cent based on the discs that could be detected by *IRAS* (e.g. Plets & Vynckier 1999), an additional cold disc population (i.e. one that *IRAS* could not detect) with the same incidence rate found for our Lindroos sample would mean that the true disc fraction could have been underestimated by a factor of 2. However, it must be remembered that our sample is biased towards young stars. This may be particularly relevant, since TWA7 is also young at  $\sim 10$  Myr (Webb et al. 1999). However, this may be observational bias, since out of the three submillimetre surveys we know about that were undertaken without selection towards stars with *IRAS* excesses (this work; Zuckerman et al., in preparation; Greaves et al., in preparation) two were specifically directed towards young stars.

This does, however, raise the question of whether these discs are (a) debris discs or (b) protoplanetary remnants. The distinction lies in whether these dust discs must be continually replenished from the breakup of a population of large planetesimals. While the transition

<sup>3</sup>Note that until such observations are performed the upper limits to the temperature of this cold disc population are dependent on the assumptions concerning the shape of the SED, and that a temperature of up to  $\sim 70$  K is possible if  $\beta = 0$ .

from protoplanetary to debris disc is likely to be smooth, and there may be no definitive answer, it is important to try to make the distinction because of the implications for the incidence of these discs around older stars. If they can be shown to be protoplanetary remnants they would be much less common around more evolved stars, whereas debris discs could persist over the whole main-sequence lifetime of the parent star, albeit getting fainter or less common with age (Habing et al. 1999; Spangler et al. 2001). Also, if they can be shown to be debris discs, it implies that significant grain growth has occurred at large distances from the star.

(a) Planet formation models do predict the existence of cold debris dust rings at large distances from the star (Kenyon & Bromley 2002). In these models a collisional cascade is ignited at a given distance from the star once planetesimals in this region have grown to  $\sim 1000$  km. This makes a bright dust ring that subsequently decreases in brightness until the supply of the 1 km planetesimals that feed the cascade is exhausted. Because of the longer planetesimal growth time-scales at larger distances from the star, this means that as the system evolves we would expect to see a bright dust ring expanding out to larger radii until it reaches the edge of the disc. However, this model predicts that cold dust rings at  $> 150$  au would not occur until a few Gyr. They also do not account for the effect of the binary companion, which would stir the planetesimal population making collisions more energetic. This could help the situation by igniting a collisional cascade without having to wait for planetesimals to grow to 1000 km, although this may also hinder it by inhibiting planetesimal growth in the first place.

(b) A different model predicts the existence of cold dust rings left over from the protoplanetary disc (Clarke et al. 2001). This model was developed to explain the rapid removal on a 0.1-Myr time-scale of T Tauri discs at an age of  $\sim 10$  Myr, and shows how these time-scales can be achieved by the viscous evolution of a gas disc in conjunction with its photoevaporation by the central star. In this model it is just the disc within the gravitational radius ( $\sim 7$  au in their standard model) that is dispersed rapidly (in 0.1 Myr) at 10 Myr; the outer disc is subsequently dispersed over a  $> 10$  Myr time-scale as its inner edge expands outwards. Thus Clarke et al. predicted the existence of cold discs that would be preferentially detected in the submillimetre regime beyond  $\sim 28$  Myr, since by this time the only part of the primordial gas disc that would remain would be outside 100 au. However, a more recent study claims that the rapid clearing of the inner disc is not reproduced when account is taken for the reduction in photoionizing flux from the central source when the accretion flux is reduced as the inner disc dissipates (Matsuyama, Johnstone & Hartmann 2003). Rather this study predicts that the outer disc is dispersed at the same rate as the inner disc.

While the models provide conflicting arguments as to the likely origin of the dust, it may be possible to determine this observationally. Dust spirals in toward the central star due to the Poynting–Robertson (P-R) drag force on time-scales of  $400r^2/\alpha M_*$  yr, where  $r$  is the distance of the dust from the star in au,  $M_*$  is the mass of the star in  $M_\odot$  and the parameter  $\alpha$  is the ratio of the radiation pressure force to stellar gravity acting on the dust particles, which is a strong function of their size with smaller particles being more affected (e.g. Wyatt et al. 1999). Thus a disc that is 200–540 au from the 2.3 solar mass star HD 99803B would have a P-R drag lifetime for the smallest remnant grains ( $\alpha = 1$ ) of 7–50 Myr. As this is shorter than the age of the system of  $\sim 120$  Myr, for the disc we detected to be primordial (i.e. not second generation), and so for its constituent dust to have survived at this distance from the star over the age of the system, this dust must have  $\alpha \ll 0.1$  correspond-

ing to grains much larger than  $\sim 0.1$  mm; i.e. there can be no small ( $< 0.1$  mm) primordial grains in this cold disc.<sup>4</sup> On the other hand, such small grains are expected to be abundant in a debris disc, since they are continually replenished by the collisional destruction of larger planetesimals that have longer P-R drag lifetimes.

Thus, while we are not proposing that the size distribution of grains in primordial and debris discs should be inherently different, we note that if these discs are protoplanetary, their necessary lack of small ( $< 0.1$  mm) grains would have a potentially discernible effect on their SEDs. If protoplanetary the emission of the discs would resemble blackbody emission with  $\beta = 0$  (e.g. Fig. 3), whereas if debris discs, their emission would have a  $\beta$  closer to 1. Thus it may be possible to use a shallow submillimetre spectral slope (i.e. emission  $\propto 1/\lambda^{<2.5}$ ) to infer a lack of small grains (Dent et al. 1998; Sheret et al. in preparation) and a protoplanetary origin. Further information concerning grain size could also be derived from SED modelling if the radial location of the dust could be determined by imaging the disc emission (e.g. Wyatt & Dent 2002).

#### 6.4 Evolution of dust mass

Leaving aside the uncertainty in the origin of the emission we detected, in Fig. 4 we have plotted the dust masses from Table 2 against system age, assuming that the emission is circumstellar. This shows how the dust masses derived in this study compare with those of the discs detected around stars of different ages. While the dust mass limits achieved here vary with system distance, for all but the most distant high-mass star in our sample we have been able to rule out the presence of dust masses even an order of magnitude below the levels that are characteristic of younger ( $< 10$  Myr) pre-main-sequence (T Tauri or Herbig Ae) stars. The dust masses that were detected in this sample, on the other hand, are similar to those of the most massive debris discs. Thus there is no evidence that massive protoplanetary discs persist far beyond  $\sim 10$  Myr.

Fig. 4(c) also emphasizes how protoplanetary and debris discs appear to come from distinct populations, since there are no known discs with masses in the  $1\text{--}10 M_\oplus$  range. This implies that the evolution from protoplanetary to debris disc occurs rapidly at an age of  $\sim 10$  Myr. However, the apparent gap in the plot could, in fact, be caused by a combination of the plotting strategy and the limited number of disc masses available to be plotted. What Fig. 4 really shows is the maximum disc mass that we know exists around stars of different ages. To interpret this correctly we also need to know the fraction of stars at a given age that are plotted in this figure. Studies of young ( $< 10$  Myr) stars are biased towards either classical or weak-line T Tauris (CTTs and WTTs, respectively) found in the nearest sites of recent star formation (at  $\sim 150$  pc). The ratio of these populations (WTT/CTT) is uncertain, but could be as high as 10 (Stahler & Walter 1993). The fraction of CTTs and WTTs that have  $> 10 M_\oplus$  discs is  $\sim 50$  and  $\sim 10$  per cent, respectively (Osterloh & Beckwith 1995), and the disc fraction for CTTs (but not that of WTTs) may be higher, up to 100 per cent, when this mass limit is decreased to  $> 2 M_\oplus$  (Duvert et al. 2000). Thus the total fraction of all young ( $< 10$  Myr) stars with massive ( $> 2 M_\oplus$ ) discs could be as low as 18 per cent [i.e.  $(10 \text{ per cent} \times 10 + 100 \text{ per cent} \times 1)/11$ ]. Given that we would expect disc masses for collisionally replenished discs to decline with age  $\propto t^{-2}$  as observed (Spangler et al.

<sup>4</sup>For the  $1.6 M_\odot$  star HD 112412 dust in its disc has a P-R drag lifetime of 5–12 Myr. Similar conclusions to those for the HD 99803B disc are less certain due to the uncertainty in the age of this system.

2001), we thus might expect that, if this decline starts at  $\sim 10$  Myr, then by 70 Myr (the average age of the Lindroos sample) 18 per cent of the stars would have discs more massive than  $0.04 M_{\oplus}$ . This is consistent with our detection of  $\geq 4/22$  discs in the Lindroos sample at this level, and so from this study alone we cannot state that the disc mass decline after 10 Myr must be steeper than  $t^{-2}$ .

Rather it is possible that if CTTs and WTTs come from separate populations, and do not form an evolutionary sequence in which CTTs evolve into WTTs on short  $\sim 0.1$  Myr time-scales (Skrutskie et al. 1990; Clarke et al. 2001), then a large number of evolved CTTs could have discs with dust masses in the range  $1\text{--}10 M_{\oplus}$  and these would be detected once a larger sample of nearby young stars has been observed. Indeed, we may already have observed one, since if the emission towards HD 74067 is bound to this system, then if this system had been twice as distant (i.e. at a similar distance to the nearest  $< 10$  Myr stars), the larger contribution of the circumbinary material in the central bolometer could have resulted in the inference of a  $1\text{--}10 M_{\oplus}$  disc. Apart from this Lindroos sample, suitable young ( $\sim 10$  Myr) nearby ( $< 70$  pc) candidates include members of the  $\beta$  Pictoris moving group (Zuckerman et al. 2001a) and the TW Hydrae Association (Zuckerman et al. 2001b; Zuckerman et al., in preparation).

## 7 CONCLUSIONS

Of the 22 young stars in our sample from the Lindroos catalogue, we report the detection of submillimetre emission (detected by us using SCUBA) towards three of these stars and far-IR emission (detected by *IRAS*) towards another star.

(i) Two of the submillimetre detections (HD 112412 and 99803B) we attribute to cold ( $< 40$  K assuming  $\beta = 1$ ) circumsecondary discs, since these were not detected in the far-IR by *IRAS* and the primary falls outside the beam; these discs have masses of  $\sim 0.04$  and  $0.3 M_{\oplus}$ , respectively. We were also able to show that a cold ( $< 50$  K assuming  $\beta = 0.5$ ) circumprimary disc is present around HD 112413 with a similar mass to the circumsecondary HD 112412 disc. These detections imply that current estimates of disc fractions could be underestimated by a factor of 2 and indicate that a significant cold submillimetre disc population could be awaiting discovery in future submillimetre and far-IR surveys. It may be possible to determine whether these discs are protoplanetary remnants or debris discs once their far-IR emission and submillimetre spectral slopes have been measured, since the emission, if protoplanetary, would more closely resemble blackbody emission.

(ii) The submillimetre emission detected toward the third binary system (HD 74067) appears to be centrally peaked and extends out to  $\sim 70$  arcsec from the system. The low temperature and high density of this emission means that it is unlikely to be caused by local cirrus heated by the star. Thus this is either a system containing a cold  $0.3\text{--}M_{\oplus}$  circumstellar disc as well as a  $> 27 M_{\oplus}$  circumbinary disc/envelope extending out to  $\sim 6000$  au, or this is a chance alignment with an unrelated background object. The former interpretation would support the idea that T Tauri discs in binary systems are replenished by extended circumbinary envelopes (Prato & Simon 1997). Since we were chopping on to an extended source, it was difficult to determine the true structure of this emission, thus further mapping of this region will help determine its origin. If this emission is bound to the star this would be an extremely unusual system in that it retains a dust mass of  $\gg 1 M_{\oplus}$  until an age of  $\sim 60$  Myr.

(iii) The far-IR emission detected towards HD 1438 implies that one of the stars in this system harbours a  $107\text{--}K$ ,  $0.05\text{--}M_{\oplus}$  circumstellar disc. If circumprimary, this disc could be resolved with mid-IR imaging from an 8-m telescope.

The low inferred dust masses for this sample supports the picture that protoplanetary dust discs are depleted to the levels of the brightest debris discs ( $\sim 1 M_{\oplus}$ ) at the end of 10 Myr. However, a larger sample of young stars must be observed before anything more concrete can be said on this subject.

## ACKNOWLEDGMENTS

The JCMT is operated by the Joint Astronomy Centre, on behalf of the UK Particle Physics and Astronomy Research Council, the Netherlands Organization for Pure Research, and the National Research Council of Canada. This research has made use of the NASA/IPAC Infrared Science Archive, which is operated by the Jet Propulsion Laboratory, California Institute of Technology, under contract with the National Aeronautics and Space Administration. We would also like to thank an anonymous referee for helpful comments.

## REFERENCES

- Andre P., Montmerle T., 1994, *ApJ*, 420, 837
- Archibald E.N. et al., 2002, *MNRAS*, 336, 1
- Artymowicz P., Clampin M., 1997, *ApJ*, 490, 863
- Artymowicz P., Lubow S.H., 1994, *ApJ*, 421, 651
- Backman D.E., Paresce F., 1993, in Levy E.H., Lunine J.I., eds, *Protostars and Planets. Vol. III*. Univ. Arizona Press, Tucson, p. 1253
- Bate M.R., Bonnell I.A., 1997, *MNRAS*, 285, 33
- Beckwith S.V.W., Sargent A.I., Chini R.S., Guesten R., 1990, *AJ*, 99, 924
- Bohren C.F., Huffman D.R., 1983, *Absorption and Scattering of Light by Small Particles*. Wiley, New York
- Clarke C.J., Gendrin A., Sotomayor M., 2001, *MNRAS*, 328, 485
- Dent W.R.F., Matthews H.M., Ward-Thompson D., 1998, *MNRAS*, 301, 1049
- Dent W.R.F., Walker H.J., Holland W.S., Greaves J.S., 2000, *MNRAS*, 314, 702
- Duquennoy A., Mayor M., 1991, *A&A*, 248, 485
- Duvert G., Guilloteau S., Ménard F., Simon M., Dutrey A., 2000, *A&A*, 355, 165
- Eales S., Lilly S., Webb T., Dunne L., Gear W., Clements D., Yun M., 2000, *AJ*, 120, 2244
- Gahm G.F., Ahlin P., Lindroos K.P., 1983, *A&AS*, 51, 143
- Gahm G.F., Zinnecker H., Pallavicini R., Pasquini L., 1994, *A&A*, 282, 123
- Gaustad J.E., Van Buren D., 1993, *PASP*, 105, 1127
- Gerbaldi M., Faraggiana R., Balin N., 2001, *A&A*, 379, 162
- Greaves J.S. et al., 1998, *ApJ*, 506, L133
- Greaves J.S., Mannings V., Holland W.S., 2000, *Icarus*, 143, 155
- Habing H.J. et al., 1999, *Nat*, 401, 456
- Haisch K.E., Lada E.A., Lada C.J., 2001, *ApJ*, 553, L153
- Herbig G.H., 1978, in Mirzoya L.V., ed., *Problems of Physics and Evolution of the Universe*. Armenian Acad. Sci., Yerevan, p. 171
- Holland W.S. et al., 1998, *Nat*, 392, 788
- Holland W.S. et al., 1999, *MNRAS*, 303, 659
- Hollenbach D., Yorke H.W., Johnstone D., 2000, in Mannings V., Boss A.P., Russell S.S., eds, *Protostars and Planets, Vol. IV*. Univ. Arizona Press, Tucson, p. 401
- Hubrig S., Le Mignant D., North P., Krautter J., 2001, *A&A*, 372, 152
- Huélamo N., Brandner W., Brown A.G.A., Neuhauser R., Zinnecker H., 2001, *A&A*, 373, 657
- Huélamo N., Neuhauser R., Stelzer B., Supper R., Zinnecker H., 2000, *A&A*, 359, 227
- Jayawardhana R., Fisher S., Hartmann L., Telesco C., Pina R., Fazio G., 1998, *ApJ*, 503, L79

- Jenness T., Lightfoot J.F., 1998, in Albrecht R., Hook R.N., Bushouse H.A., eds, ASP Conf. Ser. Vol. 145, *Astronomical Analysis Software and Systems VII*. Astron. Soc. Pac., San Francisco, p. 216
- Jensen E.L.N., Akeson R.L., 2003, *ApJ*, 584, 875
- Jensen E.L.N., Mathieu R.D., Fuller G.A., 1996, *ApJ*, 458, 312
- Jewitt D.C., 1994, *AJ*, 108, 661
- Johnstone D., Hollenbach D., Bally J., 1998, 499, 758
- Kalas P., Graham J.R., Beckwith S.V.W., Jewitt D.C., Lloyd J.P., 2002, *ApJ*, 567, 999
- Kenyon S.J., Bromley B.C., 2002, *ApJ*, 577, L35
- Kenyon S.J., Hartmann L., 1995, *ApJS*, 101, 117
- Lachaume R., Dominik C., Lanz T., Habing H.J., 1999, *A&A*, 348, 897
- Lagrange A.-M., Backman D.E., Artymowicz P., 2000, in Mannings V., Boss A.P., Russell S.S., eds, *Protostars and Planets*, Vol. IV. Univ. Arizona Press, Tucson, p. 639
- Lindroos K.P., 1985, *A&AS*, 60, 183 (L85)
- Lindroos K.P., 1986, *A&A*, 156, 223 (L86)
- Lissauer J.J., 1993, *ARA&A*, 31, 129
- Mannings V., Sargent A.I., 1997, *ApJ*, 490, 792
- Martín E.L., Magazzù A., Rebolo R., 1992, *A&A*, 257, 186
- Mathis J.S., 1990, *ARA&A*, 28, 37
- Matsuyama I., Johnstone D., Hartmann L., 2003, *ApJ*, 585, L143
- Meeus G., Waters L.B.F.M., Bouwman J., van den Ancker M.E., Waelkens C., Malfait K., 2001, *A&A*, 365, 476
- Murphy R.E., 1969, *AJ*, 74, 1082
- Natta A., Grinin V.P., Mannings V., Ungerechts H., 1997, *ApJ*, 491, 885
- Nürnberg D., Chini R., Zinnecker H., 1997, *A&A*, 324, 1036
- Nürnberg D., Brandner W., Yorke H.W., Zinnecker H., 1998, *A&A*, 330, 549
- O'Dell C.R., 2001, *ARA&A*, 39, 99
- Osterloh M., Beckwith S.V.W., 1995, *ApJ*, 439, 288
- Pallavicini R., Pasquini L., Randich S., 1992, *A&A*, 261, 245
- Papaloizou J., Pringle J.E., 1977, *MNRAS*, 181, 441
- Plets H., Vynckier C., 1999, *A&A*, 343, 496
- Pollack J.B., Hollenbach D., Beckwith S., Simonelli D.P., Roush T., Fong W., 1994, *ApJ*, 421, 615
- Prato L., Simon M., 1997, *ApJ*, 474, 455
- Ray T.P., Sargent A.I., Beckwith S.V.W., Koresko C., Kelly P., 1995, 440, L89
- Scott S.E. et al., 2002, *MNRAS*, 331, 817
- Shu F.H., Adams F.C., Lizano S., 1987, *ARA&A*, 25, 23
- Skinner S.L., Brown A., Walter F.M., 1991, *AJ*, 102, 1742
- Skrutskie M.F., Dutkevitch D., Strom S.E., Edwards S., Strom K.M., Shure M.A., 1990, *AJ*, 99, 1187
- Song I., Caillault J.-P., Barrado Y Navascués D., Stauffer J.R., Randich S., 2000, *ApJ*, 532, L41
- Song I., Caillault J.-P., Barrado Y Navascués D., Stauffer J.R., 2001, *ApJ*, 546, 352
- Spangler C., Sargent A.I., Silverstone M.D., Becklin E.E., Zuckerman B., 2001, *ApJ*, 555, 932
- Stahler S.W., Walter F.M., 1993, in Levy E.H., Lunine J.I., eds, *Protostars and Planets*, Vol. III. Univ. Arizona Press, Tucson, p. 405
- Strom K.M., Strom S.E., Edwards S., Cabrit S., Skrutskie M.F., 1989, *AJ*, 97, 1451
- Sylvester R.J., Dunkin S.K., Barlow M.J., 2001, *MNRAS*, 327, 133
- Waters L.B.F.M., Waelkens C., 1998, *ARA&A*, 36, 233
- Webb R.A., Zuckerman B., Platais I., Patience J., White R.J., Schwartz M.J., McCarthy C., 1999, *ApJ*, 512, L63
- Weidenschilling S.J., Cuzzi J.N., 1993, in Levy E.H., Lunine J.I., eds, *Protostars and Planets*, Vol. III. Univ. Arizona Press, Tucson, p. 1031
- White R.J., Ghez A.M., 2001, *ApJ*, 556, 265
- Worley C.E., Douglass G.G., 1996, *A&AS*, 125, 523
- Wyatt M.C., Dent W.R.F., 2002, *MNRAS*, 334, 589
- Wyatt M.C., Dermott S.F., Telesco C.M., Fisher R.S., Grogan K., Holmes E.K., Piña R.K., 1999, *ApJ*, 527, 918
- Zuckerman B., 2001, *ARA&A*, 39, 549
- Zuckerman B., Becklin E.E., 1993, *ApJ*, 414, 793
- Zuckerman B., Song I., Bessell M.S., Webb R.A., 2001a, *ApJ*, 562, L87
- Zuckerman B., Webb R.A., Schwart M., Becklin E.E., 2001b, *ApJ*, 549, L233

This paper has been typeset from a  $\text{\LaTeX}$  file prepared by the author.